Absence of Cooling in New Zealand and the Adjacent Ocean During the Younger Dryas Chronozone

Timothy T. Barrows, *et al.*

Science **318**, 86 (2007);
DOI: 10.1126/science.1145873

year between the Pacific and Nazca plates (*23*)]. We propose that subparallel subduction of the I-P mid-ocean ridge beneath Japan at 60 to 55 Ma resulted in nearly simultaneous slab break-off along the length of the Japanese trench (~2700 km). Geological observations from southern Japan support subduction of the I-P ridge and subsequent slab break-off at 60 to 55 Ma. Evidence includes cessation of a major accretion phase in the Late Cretaceous (*24*), emplacement of the Okitsu Melange due to subduction of hot, buoyant material at 55 Ma (*24*), and cross-cutting fault fabrics that indicate a counterclockwise rotation in relative plate motions between Eurasia and the I-P plate, which are also consistent with paleothermal and paleopressure data, between 55 and 34 Ma (*25*).

Rapid subduction of the I-P ridge, over a vast distance, triggered a chain reaction of tectonic plate reorganizations. With complete subduction of the I-P ridge at 55 Ma, forces acting on the Pacific changed from ridge-push to slab-pull, which changed Pacific absolute plate motions from northwest to west (Fig. 4). The change in Pacific plate motion caused cessation of Tasman Sea spreading at ~52 Ma (*26*). Increased slab pull north of Australia, due to a westerly progression of the subducting Wharton Basin mid-ocean ridge (Fig. 4), changed Australian absolute plate motion from northwest to north. A combination of Australian and Pacific plate motion changes between 53 and 50 Ma initiated both the Tonga-Kermadec (*2*) subduction system and the Izu-Bonin-Marianas subduction systems, which initiated likely before 50 Ma, due to convergence across a fracture zone caused by the Pacific plate motion change (*27*). We suggest that the observed slowdown of sub-Pacific mantle flow at 47 Ma (*4*) was due to progressive impediment of lateral sub-Pacific mantle flow by the descending slabs of the Izu-Bonin-Marianas and Tonga-Kermadec subduction zones.

The observed opposite bend geometries of the Emperor-Hawaii seamount chain and the Pacific-Farallon fracture zones can be explained with combined absolute (relative to a fixed reference frame) and relative plate motions. Clockwise rotation of eastern Pacific absolute plate motion, combined with stable Farallon plate motion (Fig. 4), results in a clockwise bend in Pacific-Farallon fracture zones at 53 to 49 Ma (*16*). In the western Pacific, a counterclockwise change in absolute plate motion, from northwest to west due to Izanagi Ridge subduction (Fig. 4), combined with a sub-Pacific mantle flow slowdown, results in the HEB. This conceptual model is testable via three-dimensional fully dynamic mantle flow simulations.

References and Notes

1. D. L. Anderson, *Science* **293**, 2016 (2001).
2. M. Gurnis, C. Hall, L. Lavier, *Geochem. Geophys. Geosyst.* **5**, Q07001 (2004).
3. S. D. King, J. P. Lowman, C. W. Gable, *Earth Planet. Sci. Lett.* **203**, 83 (2002).
4. J. A. Tarduno *et al.*, *Science* **301**, 1064 (2003).
5. P. Molnar, J. Stock, *Nature* **327**, 587 (1987).
6. B. Steinberger, R. Sutherland, R. J. O'Connell, *Nature* **430**, 167 (2004).
7. C. A. Finn, R. D. Müller, K. S. Panter, *Geochem. Geophys. Geosyst.* **6**, Q02005 (2005).
8. D. A. Clague, G. B. Dalrymple, *U.S. Geol. Surv. Prof. Paper* **1350** (1987).
9. I. O. Norton, *Tectonics* **14**, 1080 (1995).
10. P. Wessel, Y. Harada, L. W. Kroenke, *Geochem. Geophys. Geosyst.* **7**, Q03L12 (2006).
11. W. D. Sharp, D. A. Clague, *Science* **313**, 1281 (2006).
12. S. C. Cande, E. M. Herron, B. R. Hall, *Earth Planet. Sci. Lett.* **57**, 63 (1982).
13. D. W. Caress, H. W. Menard, R. N. Hey, *J. Geophys. Res.* **93**, 2813 (1988).
14. P. F. Lonsdale, *Bull. Geol. Soc. Am.* **100**, 733 (1988).
15. A. A. Tikku, S. C. Cande, *J. Geophys. Res.* **104**, 661 (1999).
16. C. A. Finn, D. Moore, D. Damaske, T. Mackey, *Geology* **27**, 1087 (1999).
17. C. Gaina, R. D. Müller, B. Brown, T. Ishihara, S. Ivanov, *Geophys. J. Int.* **170**, 151 (2007).
18. D. T. Sandwell, W. H. F. Smith, *Geophys. J. Int.* **163**, 79 (2005).
19. D. C. Engebretson, A. Cox, R. G. Gordon, *Geol. Soc. Am. Spec. Pap.* **206**, 1 (1985).
20. C. T. Onishi, G. Kimura, *Tectonics* **14**, 1273 (1995).
21. K. Otsuki, *Island Arc* **1**, 51 (1992).
22. M. Brown, *J. Metamorphic Geol.* **16**, 3 (1998).
23. W. P. Schellart, J. Freeman, D. R. Stegman, L. Moresi, D. May, *Nature* **446**, 308 (2007).
24. S. M. Agar, R. A. Cliff, I. R. Duddy, D. C. Rex, *J. Geol. Soc.* **146**, 893 (1989).
25. J. C. Lewis, T. B. Byrne, *Tectonics* **20**, 548 (2001).
26. C. Gaina *et al.*, *J. Geophys. Res.* **103**, 12413 (1998).
27. C. E. Hall, M. Gurnis, M. Sdrolias, L. L. Lavier, R. D. Müller, *Earth Planet. Sci. Lett.* **212**, 15 (2003).
28. W. H. F. Smith, D. T. Sandwell, *J. Geophys. Res.* **99**, 21803 (1994).
29. J.-Y. Royer, N. Rollet, *Aust. J. Earth Sci.* **44**, 543 (1997).
30. S. C. Cande, D. V. Kent, *J. Geophys. Res.* **100**, 6093 (1995).
31. G. Duclaux, P. Rey, S. Guillot, R. P. Ménot, *Geology* **35**, 715 (2007).
32. R. P. Ménot *et al.*, in *Antarctica: A Keystone in a Changing World—Online Proceedings of the 10th ISAES*, A. K. Cooper et al., Eds. (USGS Open-File Rep. 2007-1047, Short Research Paper 048, 2007).

33. We thank W. Smith for providing the downward continued gravity grid. Reviews by M. Gurnis and S. Cande, as well as detailed comments on early versions of the manuscript by P. Wessel, A. Dutkiewicz, and J. Stock, improved the manuscript considerably. We acknowledge the Ministry of Natural Resources of the Russian Federation and Geoscience Australia, who funded collection of some of the new marine magnetic data used in this work.

Supporting Online Material

www.sciencemag.org/cgi/content/full/318/5847/83/DC1
Fig. S1
Tables S1 to S5
References

13 April 2007; accepted 3 September 2007
10.1126/science.1143769

Absence of Cooling in New Zealand and the Adjacent Ocean During the Younger Dryas Chronozone

Timothy T. Barrows,[1]* Scott J. Lehman,[2] L. Keith Fifield,[1] Patrick De Deckker[3]

As the climate warmed at the end of the last glacial period, a rapid reversal in temperature, the Younger Dryas (YD) event, briefly returned much of the North Atlantic region to near full-glacial conditions. The event was associated with climate reversals in many other areas of the Northern Hemisphere and also with warming over and near Antarctica. However, the expression of the YD in the mid- to low latitudes of the Southern Hemisphere (and the southwest Pacific region in particular) is much more controversial. Here we show that the Waiho Loop advance of the Franz Josef Glacier in New Zealand was not a YD event, as previously thought, and that the adjacent ocean warmed throughout the YD.

The Younger Dryas (YD) event was originally recognized in Northern Europe and the adjacent North Atlantic Ocean as an abrupt return to near full-glacial conditions between 11,000 and 10,000 radiocarbon (^{14}C) years ago, an interval defined as the YD chronozone (*1*). Layer counting of Greenland ice cores (*2*), tree ring counts (*3*), and calibration of the ^{14}C time scale (*4*) now place the event between ~12,900 and ~11,600 calendar years before the present (cal yr B.P.). Evidence for teleconnected reversals of climate at this time occurs widely in the Northern Hemisphere (*5*), whereas the transfer of the Greenland climate stratigraphy to Antarctic ice cores via measurements of globally well-mixed atmospheric CH_4 trapped within the ice show clearly that a deglacial reversal of climate warming in Antarctica [the Antarctic Cold Reversal (ACR)] ended just as the Northern Hemisphere YD began (*6*). The latter is consistent with an antiphased relation of climate between Greenland and Antarctica seen earlier

[1]Department of Nuclear Physics, Research School of Physical Sciences and Engineering, The Australian National University, Canberra, ACT 0200, Australia. [2]Institute of Arctic and Alpine Research and Department of Geological Sciences, University of Colorado, Boulder, CO 80309, USA. [3]Department of Earth and Marine Sciences, The Australian National University, Canberra, ACT 0200, Australia.

*To whom correspondence should be addressed. E-mail: Tim.Barrows@anu.edu.au

in the glacial period (*6*, *7*), most likely due to altered interhemispheric heat transport by the ocean and/or alternation of deep-water formation between hemispheres (*8*). What remains both uncertain and very controversial is the nature of the YD climate signal, if any, in the mid- to low latitudes of the Southern Hemisphere (*9*–*12*).

The strongest case for cooling in the mid-latitude Southern Hemisphere during the YD is made on the basis of the Waiho Loop advance of the Franz Josef Glacier on the west coast of South Island, New Zealand (*9*). Twenty-five pieces of wood found buried beneath till at Canavans Knob, 1.6 km behind the moraine and ranging in age from ~12,800 to ~13,400 cal yr B.P. (10,750 to 11,520 ^{14}C yr B.P.) (*9*) suggest that the Waiho Loop formed immediately after this period during the YD chronozone. Higher in the Southern Alps, a mean ^{10}Be exposure age of 11,720 ± 320 years on boulders from the Lake Misery moraines in Arthur's Pass (*13*) also appears to support the claim for a glacier advance during the YD. These ages have prompted widespread debate, both because other climate proxies such as pollen do not indicate substantial YD cooling (*10*) and because marine records in the southwest Pacific Ocean display very different deglacial climate signals (*12*, *14*, *15*).

We chose a twofold approach to reassess the status of the YD interval in the region. First, we exposure dated the Waiho Loop moraine using the cosmogenic isotopes ^{10}Be and ^{36}Cl. This method has an advantage over ^{14}C dating in that it directly dates the moraine itself. Two nuclides provide internal-age control because each nuclide is produced from different targets and is analyzed and standardized independently. We collected samples from 10 boulders spatially distributed along the moraine crest. In two cases [WH-06 and WH-07 (Table 1)], we collected samples from both ends of large boulders, and in six cases it was possible to sample for both ^{10}Be and ^{36}Cl from the same boulder. Samples were prepared with the use of established methods (*16*). In total, we determined 24 ages, including 6 independently prepared duplicates for ^{36}Cl.

The choice of production rates for calculating exposure age is critical because systematic calibration errors directly propagate into the exposure-age uncertainty. We chose production rates calibrated with the retreat of ice at the conclusion of the YD in Scotland (*17*). This ties the exposure age of the Waiho Loop with a location of known YD age, making a direct age comparison possible. Uncertainties in production-rate scaling factors due to the geomagnetic field and atmospheric thickness are small because our site is similar to the YD calibration sites in terms of age, latitude, and altitude.

Exposure-age results are presented in Table 1 and tables S1 to S4. There is a high degree of coherence between the ages, and only one boulder age falls within the YD chronozone. Statistical dispersion between the ages of duplicates, ages derived from different isotopes analyzed from the same sample, and ages of different samples from the same boulder is similar to the dispersion between the ages of the boulders themselves. One exception is boulder WH-09, where all three ages are significantly younger than the main grouping. This was the only boulder sampled with smaller blocks resting on top of it, perhaps indicating a former till cover. The ages from the other nine boulders form a population (χ^2/ν = 2.55, where ν is the number of degrees of freedom) with a weighted mean age of 10,480 ± 240 years (*18*). Therefore, ice retreated from the Waiho Loop moraine ~1100 years after the end of the YD, meaning that it cannot be a YD-associated event. The moraine is ~2300 years younger than the youngest wood recovered beneath till correlated with the moraine (*9*). Those dates may record the initial advance of the Franz Josef Glacier just before the YD and during the ACR (~14,450 to 12,900 cal yr B.P.), a possibility raised earlier by Broecker (*5*) on the basis of the older ^{14}C dates at Canavans Knob. If these dates record a full advance of ice to the Waiho Loop, then the moraine must have formed over a period of ~2300 years, explaining its large size.

To compare our exposure ages directly with those from the putative YD moraines at Arthur's Pass (*13*), we recalculated the latter using the YD ^{10}Be production rate (*19*). Four out of the five samples form a population (χ^2/ν = 0.28) with a weighted mean age of 13,420 ± 630 years (*20*). Therefore, ice retreated from the Lake Misery moraines at the end of the ACR, ~1800 years before the conclusion of the YD and ~3000 years before the Waiho Loop moraine was abandoned by ice. To validate our production-rate methodology, we recalculated the age of the Egesen moraines in Julier Pass, Switzerland, that are believed to have formed during the YD (*13*). The new weighted mean ages for the outer and inner Egesen moraines are 13,020 ± 670 and 11,410 ± 440 years (versus the originally calculated ages of 11,750 ± 240 and 10,470 ± 260 years), indicating that the glacier occupied Julier Pass during the YD. Consequently, our method confirms the age of known YD moraines in the Northern Hemisphere. Even if we applied other commonly used ^{10}Be production rates (*21*, *22*), these rates would decrease the age of the Waiho Loop boulders and increase the mismatch with the YD.

The second approach we used to detect possible cooling during the YD was to construct a new high-resolution deep-sea record of sea surface temperature (SST) 180 km west of the Waiho Loop in the Tasman Sea. Core SO136-GC11 was collected during a *Sonne* cruise on the Challenger Plateau (43° 26.40′S, 167° 51.04′E, water depth of 1556 m), north of the present-day Subtropical Front and in the same meteorological area as the glacier (*23*). We estimated SST using the alkenone-unsaturation paleotemperature technique [see supporting online material (SOM)] and the empirical temperature calibration from sediments of Müller *et al*. (*24*), which is statistically identical to the laboratory-based calibration of Prahl *et al*. (*25*). Although the absolute temperature calculated from alkenone measurements depends on the choice of calibration, the relative precision of individual measurements is high (typically 0.5°C) and sufficient to detect small relative changes in SST. The age model was constructed with the use of 13 accelerator mass spectrometry (AMS) ^{14}C dates on the planktonic foraminifera *Globorotalia inflata* back to 23,830 cal yr B.P. (Fig. 1, table S5, and SOM). Because of the proximity to outwash from coastal glaciers, sedimentation rates peaked at ~18,400 and ~27,000 to 28,000 cal yr B.P., during maximum glaciation (*26*). The alkenone-sample interval during the YD chronozone is 200 to 300 years and as little as ~20 years during the last glacial maximum (LGM).

The SST reconstruction is shown in Fig. 1, along with δ^{18}O of the planktonic foraminifera *Globigerina bulloides* from SO136-GC11, Greenland and Antarctic oxygen isotope records

Table 1. Exposure ages for boulders on the Waiho Loop. Boulder ages are error-weighted means with standard deviation of the ages. The second "^{36}Cl age" column represents a duplicate analysis. Ages are in thousands of years. ND, not done.

Sample	^{36}Cl age	^{36}Cl age	^{10}Be age	Boulder age
WH-01	11.43 ± 0.60	10.70 ± 0.91	11.29 ± 0.90	11.23 ± 0.39
WH-02	11.31 ± 0.59	ND	10.39 ± 1.01	11.08 ± 0.65
WH-03	ND	ND	10.75 ± 0.85	10.75 ± 0.85
WH-04	9.57 ± 0.52	8.52 ± 1.11	9.69 ± 0.83	9.46 ± 0.64
WH-05	ND	ND	9.12 ± 0.76	9.12 ± 0.76
WH-06*	11.11 ± 0.55	ND	ND	9.24 ± 2.14†
WH-06*	8.09 ± 0.44	ND	ND	See above†
WH-07*	8.58 ± 0.47	11.62 ± 1.33	ND	9.40 ± 1.52‡
WH-07*	10.23 ± 0.58	ND	ND	See above‡
WH-08	8.28 ± 0.47	8.90 ± 0.83	6.87 ± 1.03	8.22 ± 1.04
WH-09	5.16 ± 0.30	5.03 ± 0.55	5.32 ± 0.50	5.17 ± 0.15
WH-10	12.79 ± 0.67	10.37 ± 0.81	11.37 ± 1.76	11.77 ± 1.22

*Samples from either end of large boulders. †The above value is an average age for both WH-06 samples. ‡The above value is an average age for both WH-07 samples.

(*7*, *27*), and a nearby pollen record (*28*). The timing of full-glacial cooling and subsequent deglacial warming is very similar to that seen in the South Island pollen record, consistent with a strong influence of the adjacent ocean on the local climate (*29*). Although not yet directly dated, a rapidly fluctuating SST decline and planktonic $\delta^{18}O$ increase (cooling) began ~29,000 cal yr B.P. and reached near full-glacial temperatures ~27,000 cal yr B.P., consistent with an early glacial cooling seen in the pollen series (*28*) and the longer record of New Zealand glaciation (*30*). Similar high-amplitude SST fluctuations are seen to the east of New Zealand and in the Southern Ocean (*29*).

Despite the documented presence of high-amplitude SST variability in the early (pre-LGM) part of the record, the warming after the abrupt increase in SST at ~19,000 cal yr B.P. is monotonic. There is no discernible decrease in SST during the deglacial period, only gradual warming that peaks at ~11,400 cal yr B.P. at the conclusion of the YD. There are no short-term fluctuations late in the Pleistocene that could potentially be a YD cooling event, even allowing for generous errors in the age model. Consistent with warming in the SST series, the YD interval appears to be associated locally with a period of maximum forest growth (increasing abundance of podocarps and hardwoods, Fig. 1), not cooling. The Holocene is characterized by a continuous SST decline to the present, seen also in the tropical western Pacific Ocean (*31*). This is consistent with late Holocene neoglaciation in New Zealand, including in the valley behind the Waiho Loop moraine (*32*).

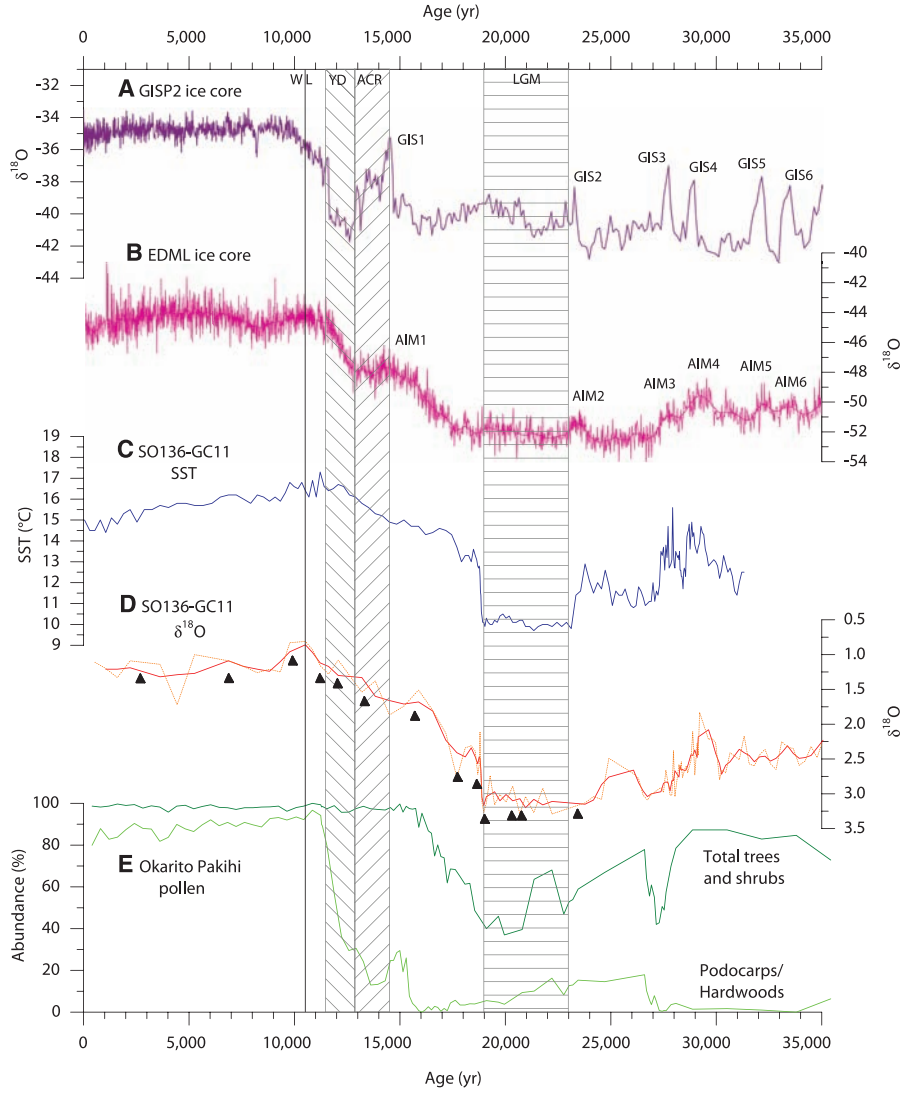

Fig. 1. (**A**) Greenland Ice Sheet Project 2 (GISP2) ice core $\delta^{18}O$ record (*27*). GIS, Greenland Interstadial. (**B**) Antarctic European Project for Ice Coring in Antarctica (EPICA) Dronning Maud Land (EDML) ice core $\delta^{18}O$ record (*7*) (solid line is a spline fit). AIM, Antarctic isotope maximum. (**C**) Alkenone-derived SST record of SO136-GC11. (**D**) Planktonic oxygen isotope record of SO136-GC11 (solid line is a three-point running mean). Triangles show the position of ^{14}C dates. (**E**) Pollen abundance of podocarps and hardwoods together with that of total trees and shrubs from Okarito Pakihi (*28*), located about 12 km from the Waiho Loop. YD, Younger Dryas chronozone; WL, age of the Waiho Loop.

The new and revised exposure ages presented here overturn evidence for glacier advance in New Zealand during the YD chronozone, previously considered to be the strongest basis for cooling in the Southern Hemisphere at this time (*5*). The possibility of glacier advance of the Franz Josef Glacier during the ACR cannot be ruled out, but we show that retreat from the Waiho Loop occurred several millennia later. Glacier retreat from the moraines at Arthur's Pass occurred much earlier. The upwind SST record indicating progressive warming during both the ACR and the YD is not readily consistent with regional forcing of coordinated glacier advance at either time and probably points to more local controls on glacier mass balance, especially for the Franz Josef Glacier (*33*). The absence of YD cooling in New Zealand increasingly calls into question its presence within the Southern Hemisphere, especially in mid-latitudes where there is little or no physical basis for climate teleconnection with the North Atlantic region.

References and Notes

1. J. Mangerud, S. T. Andersen, B. E. Berglund, J. J. Donner, *Boreas* **3**, 109 (1974).
2. S. O. Rasmussen *et al.*, *J. Geophys. Res.* **111**, D06102 (2006).
3. B. Becker, B. Kromer, *Radiocarbon* **28**, 961 (1986).
4. K. A. Hughen, J. R. Southon, S. J. Lehman, J. T. Overpeck, *Science* **290**, 1951 (2000).
5. W. S. Broecker, *Science* **300**, 1519 (2003).
6. T. Blunier, E. J. Brook, *Science* **291**, 109 (2001).
7. EPICA Community Members, *Nature* **444**, 195 (2006).
8. T. M. Marchitto, S. J. Lehman, J. D. Ortiz, J. Flückiger, A. van Geen, *Science* **316**, 1456 (2007); published online 10 May 2007 (10.1126/science.1138679).
9. G. H. Denton, C. H. Hendy, *Science* **264**, 1434 (1994).
10. C. Singer, J. Shulmeister, B. McLea, *Science* **281**, 812 (1998).
11. F. Lamy *et al.*, *Science* **304**, 1959 (2004).
12. T. Correge *et al.*, *Nature* **428**, 927 (2004).
13. S. Ivy-Ochs, C. Schlüchter, P. W. Kubik, G. H. Denton, *Geogr. Ann. Ser. A Phys. Geogr.* **81**, 313 (1999).
14. K. Pahnke, J. P. Sachs, *Paleoceanography* **21**, PA2003 (2006).
15. K. Pahnke, R. Zahn, H. Elderfield, M. Schulz, *Science* **301**, 948 (2003).
16. T. T. Barrows, J. O. Stone, L. K. Fifield, R. G. Cresswell, *Quat. Sci. Rev.* **21**, 159 (2002).
17. Materials and methods are available as supporting material online.
18. The χ^2/ν statistic > 1 suggests that there may be former shielding on some of the younger boulders or earlier exposure on some of the older boulders, increasing the overall scatter in the data. Eliminating some of the younger ages would increase the age of the moraine but would not affect the conclusion that the moraine is younger than 11,600 years.
19. J. O. Stone, C. K. Ballantyne, L. K. Fifield, *Geology* **26**, 587 (1998).
20. The inclusion of the fifth younger age increases the χ^2/ν statistic to 1.5 and does not change the conclusion (weighted mean age for the moraine becomes 12,720 ± 550 years).
21. K. Nishiizumi *et al.*, *J. Geophys. Res.* **94**, 17907 (1989).
22. P. W. Kubik, S. Ivy-Ochs, *Nucl. Instrum. Methods* **B223–B224**, 618 (2004).
23. B. Anderson, W. Lawson, I. Owens, B. Goodsell, *J. Glaciol.* **52**, 597 (2006).
24. P. J. Müller, G. Kirst, G. Ruhland, I. von Storch, A. Rosell-Melé, *Geochim. Cosmochim. Acta* **62**, 1757 (1998).

25. F. G. Prahl, L. A. Muehlhausen, D. L. Zahnle, *Geochim. Cosmochim. Acta* **52**, 2303 (1988).
26. R. P. Suggate, P. C. Almond, *Quat. Sci. Rev.* **24**, 1923 (2005).
27. P. M. Grootes, M. Stuiver, J. W. C. White, S. Johnsen, J. Jouzel, *Nature* **366**, 552 (1993).
28. M. J. Vandergoes *et al.*, *Nature* **436**, 242 (2005).
29. T. T. Barrows, S. Juggins, P. De Deckker, E. Calvo, C. Pelejero, *Paleoceanography* **22**, PA2215 (2007).
30. S. C. Porter, *Quat. Res.* **5**, 27 (1975).
31. L. Stott *et al.*, *Nature* **431**, 56 (2004).
32. S. C. Porter, *J. Quat. Sci.* **15**, 395 (2000).
33. Moraines similar to the Waiho Loop are absent from adjacent glacier-occupied valleys. Nonetheless, circulation patterns are closely linked to glacier advance and retreat in New Zealand (*34*), so it is likely that persistent southwesterly circulation occurred at the time of the deposition of the Waiho Loop.
34. P. D. Tyson, A. P. Sturman, B. B. Fitzharris, S. J. Mason, I. F. Owens, *Int. J. Climatol.* **17**, 1499 (1997).
35. We thank H. Scott-Gagan, J. Cali, and M. Gagan (Research School of Earth Sciences, Australian National Univ.) for helping to prepare the oxygen isotope data; A. Crotwell [Institute of Arctic and Alpine Research (INSTAAR), Univ. of Colorado] for helping to prepare alkenone samples; J. Turnbull (INSTAAR Laboratory for AMS Radiocarbon Preparation and Research, Univ. of Colorado) for the preparation of ^{14}C samples for AMS; J. Thiede, S. Nees, and K. Swanson, who were instrumental in obtaining core SO136-GC11; and S. Tims for helping to collect the AMS data. This work was supported by Australian Research Council grants [to T.T.B. (DP0557143) and P.D.D.] and NSF grant OCE 0081257 (to S.J.L.).

Supporting Online Material
www.sciencemag.org/cgi/content/full/318/5847/86/DC1
Materials and Methods
Fig. S1
Tables S1 to S5
References

30 May 2007; accepted 30 August 2007
10.1126/science.1145873

Toward Direct Measurement of Atmospheric Nucleation

Markku Kulmala,[1]* Ilona Riipinen,[1] Mikko Sipilä,[1] Hanna E. Manninen,[1] Tuukka Petäjä,[1] Heikki Junninen,[1] Miikka Dal Maso,[1] Genrik Mordas,[1] Aadu Mirme,[2] Marko Vana,[1,2] Anne Hirsikko,[1] Lauri Laakso,[1] Roy M. Harrison,[3] Ian Hanson,[3] Carl Leung,[3] Kari E. J. Lehtinen,[4] Veli-Matti Kerminen[5]

Atmospheric aerosol formation is known to occur almost all over the world, and the importance of these particles to climate and air quality has been recognized. Although almost all of the processes driving aerosol formation take place below a particle diameter of 3 nanometers, observations cover only larger particles. We introduce an instrumental setup to measure atmospheric concentrations of both neutral and charged nanometer-sized clusters. By applying the instruments in the field, we come to three important conclusions: (i) A pool of numerous neutral clusters in the sub–3 nanometer size range is continuously present; (ii) the processes initiating atmospheric aerosol formation start from particle sizes of ~1.5 nanometers; and (iii) neutral nucleation dominates over the ion-induced mechanism, at least in boreal forest conditions.

Formation of new atmospheric aerosol particles (diameter of 3 to 10 nm) by nucleation and subsequent growth has been observed in a wide variety of low- and high-altitude locations (*1*). Once the formed particles grow further in size, they may participate in cloud formation and influence the regional or even global radiation balance and ultimately climate. On more local scales, these particles may be deleterious to human health and impair visibility.

Despite the growing list of locations where frequent aerosol formation has been observed, the overall magnitude of this source is still very poorly understood compared with that of any other major source generating particles into the atmosphere. There are at least two reasons for this. First, atmospheric aerosol formation is driven by processes taking place below a 3-nm particle diameter, which is outside the range of most measuring devices in use. Second, the nucleation mechanism initiating aerosol formation is likely to vary with location and atmospheric conditions. Proposed atmospheric nucleation mechanisms include kinetic (or barrierless), binary, ternary, and ion-induced (or ion-mediated) nucleation (*1*–*3*), some of which might further be affected by meteorological processes such as turbulent fluctuations, atmospheric waves, and mixing (*4*, *5*). Most nucleation mechanisms have been thought to involve gaseous sulfuric acid, even though nucleation taking place in association with clouds and in coastal areas could be induced by water-insoluble (*6*) and iodine compounds (*7*), respectively.

Recently it was suggested that the formation of new atmospheric aerosol particles is connected with the existence of thermodynamically stable 1- to 2-nm clusters (*8*), formed in the atmosphere by some nucleation mechanism. From a physical standpoint, two very different cluster types in the sub–3 nm size range can be distinguished: charged (air ions or ion clusters) and neutral species. The existence of atmospheric ion clusters as small as 0.5 to 1 nm in diameter has been known for decades, and measurements with ion spectrometers, such as the Air Ion Spectrometer (AIS) and Balanced Scanning Mobility Analyzer (BSMA), have demonstrated that such clusters are present almost all the time (*9*). The production rates of ion clusters are, however, generally too low to explain the observed aerosol-formation rates (*10*).

In view of the insufficient numbers of ion clusters, the key to understanding atmospheric aerosol formation is clearly the presence of neutral clusters. Theoretical arguments predict the existence of such clusters (*8*, *11*) and suggest that

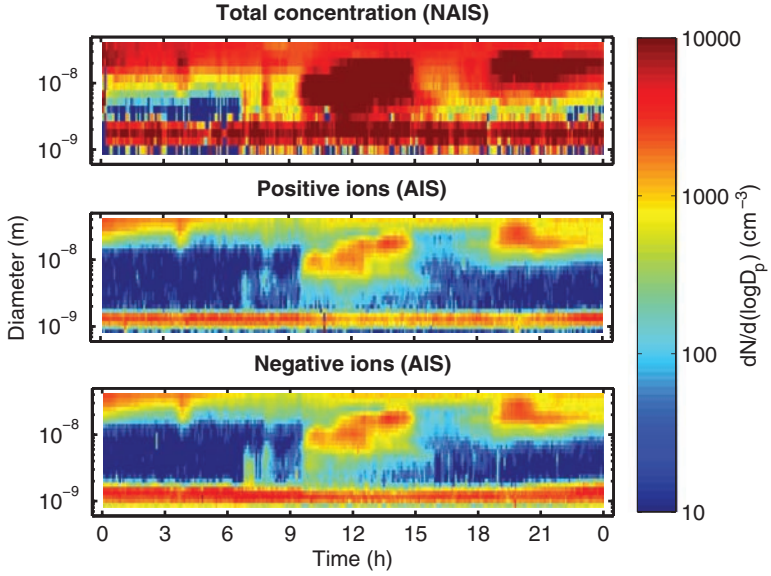

Fig. 1. Evolution of particle number size distribution measured with the NAIS on a particle formation event day (23 April 2006) in Hyytiälä, Finland.

[1]Department of Physical Sciences, University of Helsinki, Post Office Box 64, FI-00014, Helsinki, Finland. [2]Institute of Environmental Physics, University of Tartu, Ülikooli 18, EE-50090, Tartu, Estonia. [3]Division of Environmental Health and Risk Management, School of Geography, Earth and Environmental Sciences, University of Birmingham, Edgbaston, Birmingham B15 2TT, UK. [4]Department of Physics, University of Kuopio and Finnish Meteorological Institute, Kuopio Unit, Post Office Box 1627, 70211 Kuopio, Finland. [5]Finnish Meteorological Institute, Post Office Box 503, FI-00101, Helsinki, Finland.

*To whom correspondence should be addressed. E-mail: kulmala@pcu.helsinki.fi